We are IntechOpen, the world's leading publisher of Open Access books Built by scientists, for scientists

6,900
Open access books available

186,000
International authors and editors

200M
Downloads

Our authors are among the

154
Countries delivered to

TOP 1%
most cited scientists

12.2%
Contributors from top 500 universities

CLARIVATE ANALYTICS
BOOK CITATION INDEX
INDEXED

WEB OF SCIENCE™

Selection of our books indexed in the Book Citation Index
in Web of Science™ Core Collection (BKCI)

Interested in publishing with us?
Contact book.department@intechopen.com

Numbers displayed above are based on latest data collected.
For more information visit www.intechopen.com

Variations of the Absorption of Chromophoric Dissolved Organic Matter in the Pearl River Estuary

Xia Lei, Jiayi Pan and Adam Thomas Devlin

Abstract

Analysis of in-situ measurements during a spring cruise survey in the Pearl River Estuary (PRE) reveals that, controlled by the two-layer gravitational circulation, chromophoric dissolved organic matter (CDOM) absorption shows a clear horizontal distribution pattern at both water surface and bottom, with higher CDOM absorption and lower spectral slope in the northwestern estuary, and a reversed pattern in the southeastern estuary and near the Hong Kong waters. The surface CDOM has higher absorption and lower spectral slope than the bottom. Horizontal transport is suggested to be the dominant hydrodynamic mechanism affecting CDOM distribution pattern in the PRE. With a regional algorithm tailored for the PRE CDOM absorption retrieval, a time series of CDOM absorption and spectral slope in the PRE and the Hong Kong waters in spring from 2012 to 2018 is produced based on satellite images obtained by four sensors with different spatial and spectral resolutions: the Visible Infrared Imaging Radiometer Suite (VIIRS), the Ocean and Land Colour Instrument (OLCI), the Hyperspectral Imager for the Coastal Ocean (HICO), and the Operational Land Imager (OLI). A correlation is revealed between the multi-temporal CDOM absorption and the monthly averaged river discharge, indicating the capability of CDOM ocean color products in identifying hydrodynamic processes in estuaries and coastal waters.

Keywords: chromophoric dissolved organic matter, absorption, ocean color, time series, Pearl River Estuary

1. Introduction

The chromophoric (or colored) dissolved organic matter (CDOM) is the light-absorbing part of the dissolved organic matter (DOM) in natural waters, which may cause a yellow or brown water color at high concentrations [1]. Chemically, CDOM refers to an ensemble of structures including carboxylic acids and carboxyl-rich alicyclic molecules, substituted phenols, ketones, aldehydes, quinones, carbohydrates, saturated and unsaturated hydrocarbons, and nitrogenous material [2].

The major sources of CDOM in the marine environment are terrestrial-derived, oceanic-produced, or sediment-introduced [1]. The terrestrial CDOM is originally synthesized by land and water plants, subsequently processed and modified in limnic systems and eventually exported to coastal waters. The oceanic CDOM is originally fixed by marine plants or phytoplankton, produced by heterotrophic and

autotrophic organisms, or formed by photooxidation of colorless DOM [3–5]. The sediment CDOM is often observed in coastal waters and shelf seas where sediment resuspension, hypoxia events or hydrothermal events occur [6–8].

The processes involved in the removal of CDOM in nature waters include photodegradation and microbial activities. The photochemical reaction triggered by CDOM absorption of high-energy (low wavelength) light can have great impacts on biogeochemical processes and water ecology [9–11]. Heterotrophic microbes either incorporate or respire organic matter and modify CDOM into labile DOM, which are rapidly degraded in the process [12].

Estuaries and coastal waters are very productive systems, where high loading of terrestrial CDOM and high local production are mixed, processed and exported to shelf seas [1]. Therefore, a better understanding of CDOM variation in estuaries and coastal waters can help estimating the oceanic carbon budget and evaluating the anthropogenic impacts on marine environments and global climate change. Furthermore, in estuarine and coastal waters, CDOM absorption usually co-varies with salinity. Variation of CDOM absorption can be used as a tracer of water mass mixing in near shore waters [13]. Investigating and explaining CDOM variations are therefore crucial for understanding various processes in the aquatic environment.

The Pearl River Estuary (PRE) is located on the southern coast of Guangdong, China (22–22.75°N, 113.5–114°N) (**Figure 1**), adjacent to the Northern South China Sea (NSCS). Its major part, the Lingdingyang Estuary, has a trumpet-like shape, with four gates (Humen, Jiaomen, Hongqili, and Hengmen) on the west side of the upper estuary, discharging freshwater of 6.83×10^{10} m^3 into the NSCS every year [14]. The eastern side, however, has two deep channels, along which the coastal sea water can flood into [15]. The various water masses with complex properties make it difficult to interpret the CDOM variations in the estuary.

Furthermore, as China's second largest river in terms of water discharge, the Pearl River has an annual mean discharge of 10,000 m^3 s^{-1} [15–17]. A significant seasonal variation exists in the Pearl River discharge. Therefore, the optical properties of the estuarine water can be strongly influenced by river discharge, especially during the wet season [15], which leads to distinctive characteristics when interpreting and quantifying CDOM variations in the PRE in different seasons.

Studies on CDOM absorption in the PRE last for decades. Previous studies of CDOM optical properties have covered the entire estuary in different seasons of the year, but detailed picture of CDOM variation in the estuary remains poorly understood, the dynamics of CDOM optical properties under control of multiple
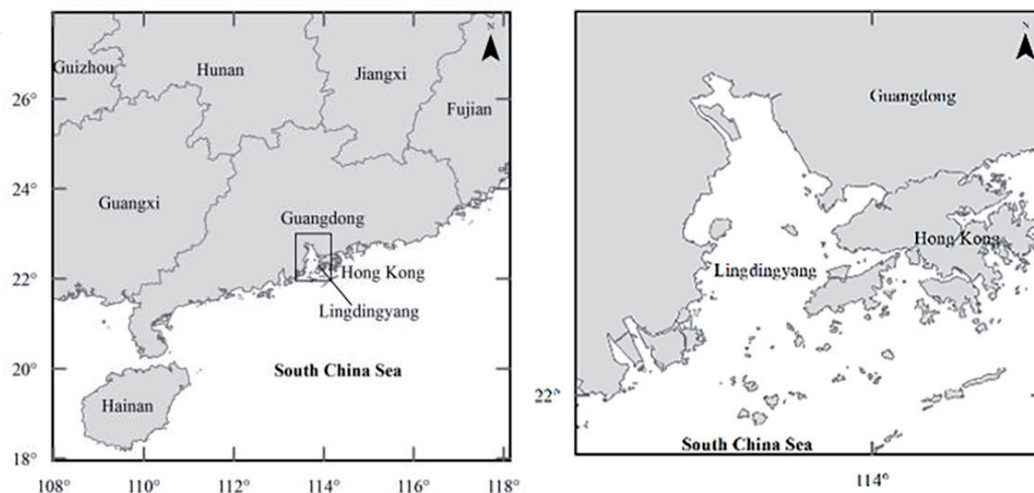

Figure 1.
Location of Lingdingyang Estuary, the major part of the Pearl River Estuary.

hydrodynamic and biogeochemical processes are not yet to be revealed satisfactorily, and the ocean color algorithms for CDOM optical property retrieval with high reliability are still needed to be developed, as well as the CDOM ocean color products with high spatial and temporal resolutions. Therefore, a comprehensive investigation of CDOM optical properties synthesizing advantages of in-situ observations and ocean color interpretations is still in necessity.

The aim of this research is to enhance the understanding of the spatial and temporal variations of CDOM optical properties in the PRE through analyzing in-situ measurements and interpreting satellite ocean color observations. The horizontal and vertical variations of CDOM absorption in the PRE are depicted based on dense and detailed in-situ observations and the dominant driven forces affecting the variations are discriminated. Spatial and temporal variations of CDOM optical properties in the PRE are analyzed based on the CDOM products derived from multi-source ocean color data with complemented spatial and temporal resolutions.

2. Materials and methods

2.1 In-situ observations

Generally, the absorption coefficient ($a_g(\lambda)$, m^{-1}) is a direct measure of CDOM absorptivity. The spectrum of a_g usually spans from ultraviolet band to red band. The spectral shape is unstructured and typically decreases with increasing wavelength in an exponential fashion (Eq. (1)) [18–23].

$$a_g(\lambda) = a_g(\lambda_0) \exp\left[-S_g(\lambda - \lambda_0)\right],$$ (1)

where λ_0 is the reference wavelength, and S_g is the spectral slope, describing the decreasing rate of the spectrum.

The absorptivity of CDOM is first measured on a spectrophotometer as absorbance ($A(\lambda)$), a unit-less ratio of spectral radiant power transmitted through the sample across a path length (L) [24]. $A(\lambda)$ is then converted to the (Napierian) absorption coefficient ($a_g(\lambda)$) according to Eq. (2):

$$a_g(\lambda) = 2.303 A(\lambda)/L.$$ (2)

Typically, measurements are performed using a long-path length quartz cuvette (e.g., 0.1 m) or a liquid core waveguide (0.5–5 m) with submicron-filtered (0.2 or ~0.7 μm) seawater. In low-CDOM waters, measurement of the absorption spectrum of CDOM using a conventional spectrophotometer is challenging. Due to the exponential decline of absorption with increasing wavelength, absorbance values can fall below the detection threshold of the detectors used, typically 0.03–0.06 m^{-1} [25]. Devices with longer effective path lengths, such as reflective tube absorption meters (up to 25 cm [26]), liquid waveguide cells (up to 200 cm [27, 28]), and integrating cavity meters (up to 25 m [29]) attempt to resolve this problem.

A cruise was implemented in the PRE previously from 2 to 12 May 2014. A total of 148 water samples were collected (**Figure 2**) from the water surface (with sampling depth of 0 and 1 m) and the bottom (with sampling depth 1 m above the bottom). CDOM absorbance ($A(\lambda)$) was measured in a 10-cm quartz cell using a Shimadzu UV-2550 spectrophotometer. The absorption coefficient ($a_g(\lambda)$) is calculated at 1 nm interval from 250 to 700 nm according to Eq. (2). Spectral slope, S_g, over wavelength range of UV (250–400 nm), noted as $S_g(250-400)$, is used as a
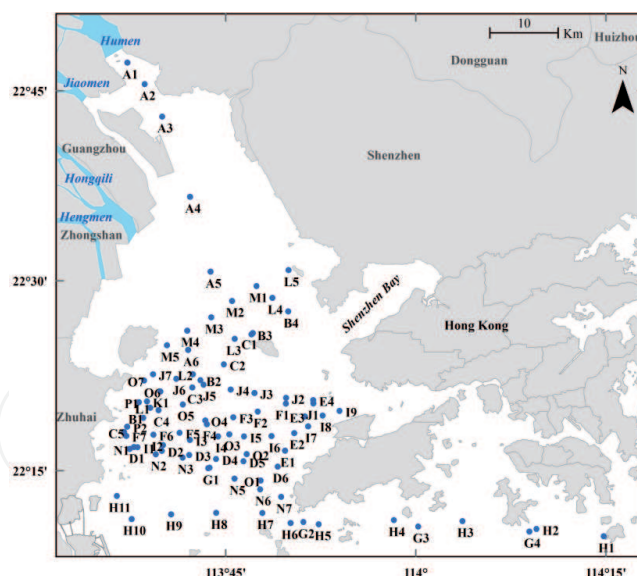
Figure 2.
Location of the sampling stations in the May 2014 cruise in the Pearl River Estuary.

representative of CDOM spectral slope when analyzing the spatial heterogeneity of CDOM [30].

In addition to the spectroscopic analysis of CDOM absorption, in-situ measurements of remote sensing reflectance in visible range (400–900 nm) are also conducted.

2.2 Satellite imagery

The in-situ measurements provide detailed observations on CDOM optical properties. However, the spatial and temporal resolutions of in-situ observations are always limited by high costs in the survey implementation. The satellite imagery can offer better temporal and spatial coverage with high efficiency and low cost. Therefore, space-born and airborne sensors have been used to monitor spectral properties of natural waters for over four decades, and ocean color remote sensing has become an important technology to study water environment.

Nevertheless, the applicability of satellite observation depends on the reliability of CDOM ocean color algorithms. The spectral properties of water bodies may change substantially with geographical locations and time. The color (spectrum) of water can be used to estimate concentrations of optically active constituents in water, such as the phytoplankton, suspended solids, and CDOM based on effective ocean color algorithms.

A regional algorithm for CDOM absorption estimation from satellite ocean color imagery is developed for the spring PRE (Eqs. (3)–(5)), which derives CDOM UV absorption and spectral slope from the visible remote sensing reflectance [$R_{rs}(\lambda)$], which is established based on the in-situ measured above water remote sensing reflectance (**Figure 3**). The algorithm is with an overall mean absolute percentage difference (MAPD) of ~30 and ~5% for the estimation of CDOM absorption and the spectral slope over 250–450 nm, respectively.

$$a_g(290) = 108.2\,R_{rs}(596) - 0.5324 \tag{3}$$

$$R_{rs}\_Gradient = [R_{rs}(max) - R_{rs}(min)]/[\lambda(max) - \lambda(min)] \tag{4}$$

$$S_g(250{-}400) = 0.01187\,R_{rs}\_Gradient^{-0.1741} \quad\quad (5)$$

Using all available satellite image data obtained by four ocean color sensors with different spatial and spectral resolutions: the Visible Infrared Imaging Radiometer Suite (VIIRS) on board Suomi National Polar-orbiting Partnership (Suomi NPP), the Ocean and Land Colour Instrument (OLCI) on board Sentinel-3A (S3A), the Hyperspectral Imager for the Coastal Ocean (HICO) integrated in the International Space Station (ISS) Window Observational Research Facility (WORF), and the Operational Land Imager (OLI) on board Landsat 8 (LS8) (**Table 1**), a time series of CDOM absorption and spectral slope in the PRE and the Hong Kong waters in spring from 2012 to 2018 is produced. Relevant factors related to the temporal variation of CDOM absorption and spectral slope are analyzed.

To match the season of the in-situ observations in this study, a set of satellite images acquired in spring (April and May) from 2012 to 2018 is selected for the application of the developed algorithm. For the OLI data with a 16-day revisit cycle, the time constraint is relaxed to March and June. The study area covers 22° and 23°N, 113.5° and 114.5°E. The images with cloud coverage below 20% are downloaded (see **Tables 2** and **3** for detailed information of the available images).
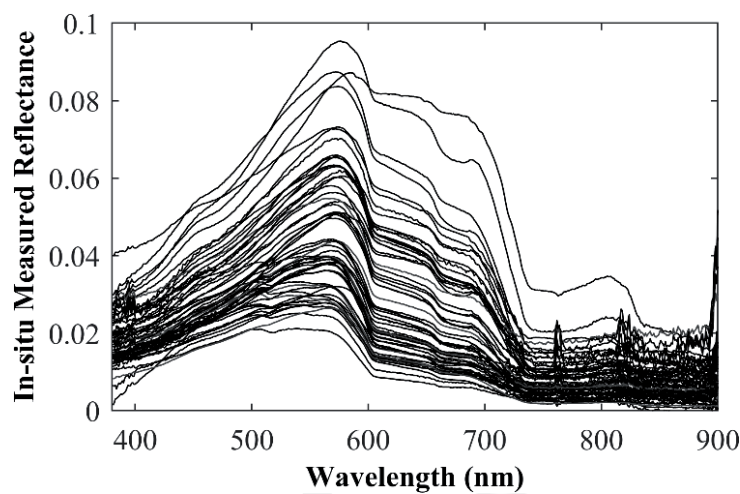

Figure 3.
Normalized in-situ water surface reflectance in 380–900 nm measured by an Ocean Optics 4000 spectrometer using above-water method.

Sensor	VIIRS	OLCI	HICO	OLI
Location	SNPP	Sentinel-3	ISS	Landsat 8
Data period	Jan 2010 to Now	Oct 2016 to Now	Sep 2009 to Sep 2014	Feb 2013 to Now
Number of bands	22	21	128	9
Spectral ranges (nm)	402–12,490	400–1020	353–1080	435–2294
Spatial resolution (m)	375/750/1000	300	100	15/30
Revisit days	1	~2	~10	16

Table 1.
The properties of ocean color remote sensors utilized in this paper.

Sensor	VIIRS	OLCI	HICO	OLI
Data period	Jan 2010 to Now	Oct 2016 to Now	Sep 2009 to Sep 2014	Feb 2013 to Now
Years searched	2012–2018	2017–2018	2012–2014	2013–2018
Months searched	Apr to May	Apr to May	Apr to May	Mar to Jun
Available images	19	5	1	8

Table 2.
Satellite images used for ocean color application.

Sensor	Acquisition time						
	2012	2013	2014	2015	2016	2017	2018
VIIRS	Apr10 May07 May23	Apr20 Apr09 May30 May31	Apr05 Apr15	Apr13 Apr14 Apr24 Apr30	Mar26	Apr02 Apr29 May31	Apr01 Apr10
OLCI						Apr01 Apr02 Apr29	Apr04 Apr08
HICO		Apr20					
OLI			Jun09	Jun12 Jun28	Mar26 May29	Apr30	Apr01 May03

Table 3.
Acquisition time of the available images.

Sensor	Spectral bands in visible range (nm)	$R_{rs}(596)$
VIIRS	412/445/488/555/672	[0.66B(555) + 0.34B(672)]/2
OLCI	400/412.5/442.5/490/510/560/620/665/673.75/681.25	[B(560) + B(620)]/2
HICO	404–696 (52 bands with interval of ~5.7 nm)	[B(593) + B(599)]/2
OLI	433–453/450–515/525–600/630–680	B3 (525–600)

Table 4.
The criterion used to match $R_{rs}(596)$ with the bands of four sensors.

Eq. (3) is applied to derive $a_g(290)$ from the selected satellite images. The $R_{rs}(596)$ is matched to the bands of the four sensors by the criteria listed in **Table 4**. When retrieving $S_g(250–400)$, considering the available spectral range of the satellite imagery and the performance of atmospheric correction, the lower ends for R_{rs} gradient calculation (the λ_{min} in Eq. (4)) are set as 445, 415.5, 400, and 443 nm for the VIIRS, HICO, OLCI and OLI data, respectively. The range for the R_{rs} maximum is limited below 700 nm for all sensors. $S_g(250–400)$ is afterward derived from R_{rs} gradient by Eq. (5).

3. Results

Figures 4 and **5** present time-series products of ocean color-retrieved CDOM absorption ($a_g(290)$) and spectral slopes ($S_g(250–400)$) from 2012 to 2018, which are derived from the satellite images listed in **Table 3** using Eqs. (3)–(5). All the products can capture the general distribution pattern of CDOM in the PRE,
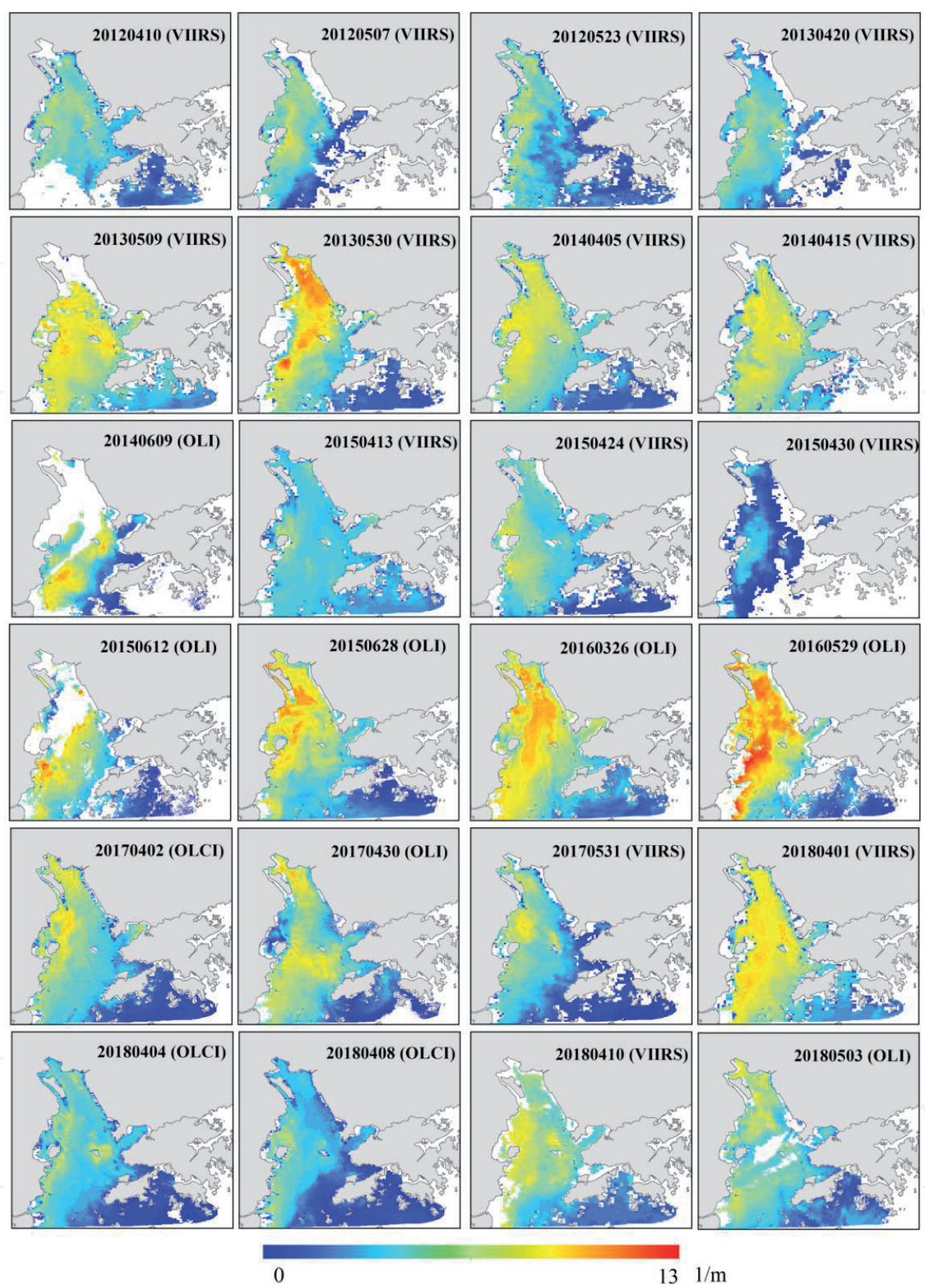
Figure 4.
Time-series of CDOM absorption ($a_g(290)$) in the PRE in spring in 2012–2018 derived from VIIRS, OLCI, HICO, and OLI.

showing the gradual decrease of absorption and the increase of spectral slope along the northwest to southeast direction.

In addition to the clear and consistent trend illustrated in **Figures 4** and **5**, the quantitative variations of CDOM absorption and spectral slope with time are also remarkable. The temporal fluctuation is especially evident in the upper and western PRE, where the water properties are greatly influenced by freshwater discharge, especially during the flooding season.
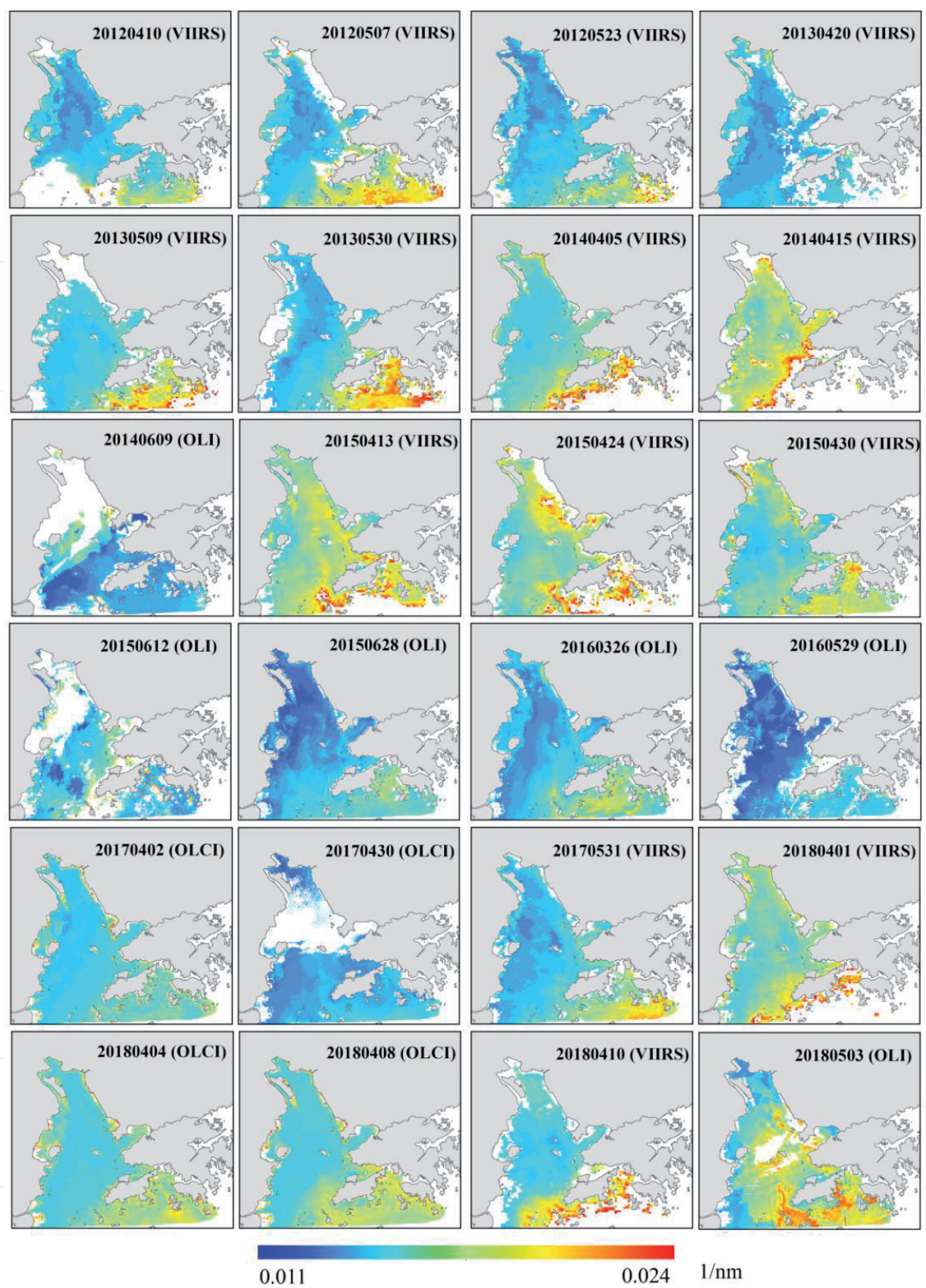
Figure 5.
Time-series of spectral slope of CDOM absorption ($S_g(250–400)$) in the PRE in spring in 2012–2018 derived from VIIRS, OLCI, HICO and OLI.

Source and removal are the two major aspects that control and balance the CDOM absorption budget in nature waters. In open oceans, phytoplankton production and upwelling of deep water can bring new CDOM into upper layer to elevate CDOM absorption in surface water, while the photobleaching and high stratification can strongly decrease the absorptivity of surface CDOM and increase the spectral slope. In estuaries and coastal waters, the most distinctive condition different from the open oceans is the terrestrial input, which is a significant source of organic
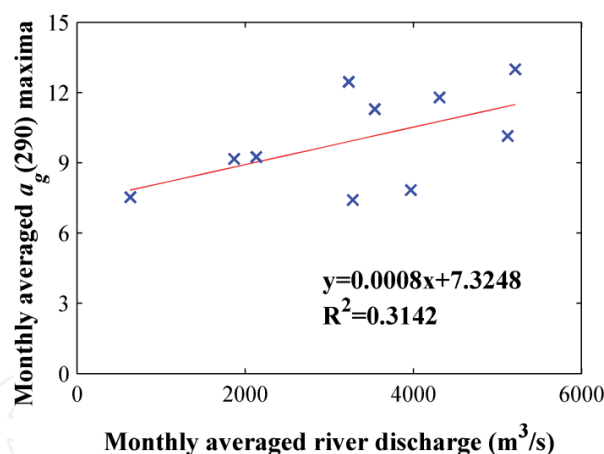
Figure 6.
Correlation between the monthly averaged river discharge of the sum of values measured by two gauging stations (Boluo and Shijiao) and the monthly averaged $a_g(290)$ maxima from the CDOM Ocean color products.

matter in surface water, and leads to the highest variation of CDOM concentration in the region [1]. Therefore, in estuaries and coastal waters, river flow is always an important factor influencing the temporal variation of CDOM absorption during the wet season.

A positive correlation between the monthly averaged river discharge and the monthly averaged $a_g(290)$ maxima from the CDOM ocean color products is shown in the PRE (**Figure 6**), suggesting the high CDOM absorption in the PRE is always associated with high river flow. This pattern is especially typical in spring, when the Pearl River enters the flood season, and the river discharge can dramatically increase after a heavy rainfall. As a contrast to the high river flow, the existing CDOM in surface water of the PRE can be rapidly photodegraded or microbial consumed under the low river discharge with limited inputs of new CDOM, resulting in low level of CDOM absorption and large value of spectral slopes. In this point of view, the time-series of CDOM absorption can be well correlated with river discharge, and therefore is a good indicator of estuarine hydrodynamic conditions.

4. Discussion

For dissolved matter in water, the variation of CDOM is greatly influenced by hydrodynamic conditions, such as horizontal transport and vertical mixing. The PRE circulation is dominated by the gravitational exchange current with the surface freshwater flowing seaward in the surface, mainly on the west side, and the compensated seawater in the lower layer flowing landward along the east coast [31, 32].

As illustrated by in-situ observations and satellite interpretation, CDOM shows the strongest absorption and lowest spectral slope at the head of the estuary (Station A1, A2 and A3) (**Figures 4** and **5**). Water in this region comes from the discharge of the Humen and Jiaomen Gates (**Figure 2**), carrying abundant dissolved organic materials. These CDOM components with complex composition are then transported seaward along the west coast, causing the western estuary to have stronger CDOM absorption and lower spectral slope than the eastern estuary, where the intrusive seawater brings large amount of marine CDOM with lower absorption and higher spectral slope.

It has been reported that terrestrial CDOM is much more sensitive to photochemical reactions than marine CDOM [33]. DOM originating from upper streams during high-flow events is abundant in aromatic compounds, and therefore is highly susceptible to solar irradiation, which is in agreement with laboratory

experiments which reveal a high degree of riverine DOM photoreaction [34]. Thus, photodegradation can be a possible reason for the removal of terrigenous CDOM in the surface water of the PRE, therefore the decrease of CDOM absorption. Furthermore, photobleaching can convert high molecular weight CDOM species to lower molecular weight species, result in a great decrease in $a_g(295)$ than in $a_g(275)$, and consequently cause the spectral slope increase [30, 35, 36].

With respect to the ocean color applications, the spatial distribution pattern of CDOM absorption in upper layer is successfully captured by the algorithm, and the time-series CDOM variation which collaboratively changes with river discharge, is also reflected from satellite multi-senor imagery. Furthermore, the variation of CDOM spectral slope (S_g) within the PRE is depicted with very high spatial resolution, by retrieving S_g from satellite imagery pixel by pixel using Eq. (5). This can lead to much more delicate CDOM absorption products (**Figures 4** and **5**), because previous algorithms to derive CDOM absorption spectra generally use a uniform S_g for the entire water area of interest to calculate a_g [37], which is evidently unreasonable for estuarine and coastal waters, where the CDOM of different sources may have different levels of S_g.

5. Conclusion

This research analyzes the variation of the CDOM optical properties (absorption) in the PRE based on the in-situ measurements during a spring cruise survey and the ocean color interpretations. Based on a UV to visible scheme to retrieve CDOM absorption from remote sensing reflectance, the time-series product of CDOM absorption in the PRE waters is produced from satellite images with multiple spatial and spectral resolutions, and an evident correlation with the temporal variation of river discharge is captured in the time-series variation of CDOM absorption in the PRE in spring.

Acknowledgements

Appendices and nomenclature

A	absorbance
a_g	absorption coefficient of CDOM
CDOM	chromophoric dissolved organic matter
DOC	dissolved organic carbon
DOM	dissolved organic matter
HICO	hyperspectral imager for the coastal ocean
ISS	International Space Station
MAPD	mean absolute percent difference
OLCI	Ocean and Land Colour Instrument
OLI	Operational Land Imager
UV	ultraviolet
VIIRS	Visible Infrared Imaging Radiometer Suite

Author details

Xia Lei[1], Jiayi Pan[2]* and Adam Thomas Devlin[2]

1 Institute of Space and Earth Information Science, The Chinese University of Hong Kong, Shatin, Hong Kong, China

2 School of Geography and the Environment, Jiangxi Normal University, Nanchang, Jiangxi, China

*Address all correspondence to: panj@cuhk.edu.hk

IntechOpen

References

[1] Stedmon CA, Nelson NB. The optical properties of DOM in the ocean. In: Hansell D, Carlson C, editors. Biogeochemistry of Marine Dissolved Organic Matter. 2nd ed. San Diego, CA: Academic Press; 2015. 481-508 p

[2] Sharpless CM, Blough NV. The importance of charge-transfer interactions in determining chromophoric dissolved organic matter (CDOM) optical and photochemical properties. Environmental Science: Processes & Impacts. 2014;**16**:654-671

[3] Steinberg DK, Nelson NB, Carlson CA, Prusak AC. Production of chromophoric dissolved organic matter (CDOM) in the open ocean by zooplankton and the colonial cyanobacterium *Trichodesmium* spp. Marine Ecology Progress Series. 2004;**267**:45-56

[4] Kieber RJ, Hydra LH, Seaton PJ. Photooxidation of triglycerides and fatty acids in seawater: Implication toward the formation of marine humic substances. Limnology and Oceanography. 1997;**42**:1454-1462

[5] Swan CM, Nelson NB, Siegel DA, Kostadinov TS. The effect of surface irradiance on the absorption spectrum of chromophoric dissolved organic matter in the global ocean. Deep Sea Research Part I: Oceanographic Research Papers. 2012;**63**:52-64

[6] Osburn CL, Handsel LT, Mikan MP, Paerl HW, Montgomery MT. Fluorescence tracking of dissolved and particulate organic matter quality in a river-dominated estuary. Environmental Science & Technology. 2012;**46**:8628-8636

[7] Skoog A, Hall POJ, Hulth S, Paxéus N, Rutgers van der Loeff M, Westerlund S. Early diagenetic production and sediment-water exchange of fluorescent dissolved organic matter in the coastal environment. Geochimica et Cosmochimica Acta. 1996;**60**:3619-3629

[8] Yang L, Hong H, Guo W, Chen CA, Pan P, Feng C. Absorption and fluorescence of dissolved organic matter in submarine hydrothermal vents off NE Taiwan. Marine Chemistry. 2012;**128-129**:64-71

[9] Blough NV, Zepp RG. Reactive oxygen species in natural waters. In: Foote CS et al., editors. Active Oxygen in Chemistry. Glasgow, UK: Chapman & Hall; 1995. pp. 280-333

[10] Johannessen SC, Miller WL. Quantum yield for the photochemical production of dissolved inorganic carbon in seawater. Marine Chemistry. 2001;**76**:271-283

[11] Nieto-Cid M, Álvarez-Salgado XA, PÉrez FF. Microbial and photochemical reactivity of fluorescent dissolved organic matter in a coastal upwelling system. Limnology and Oceanography. 2006;**51**:1391-1400

[12] Nelson NB, Carlson CA, Steinberg DK. Production of chromophoric dissolved organic matter by Sargasso Sea microbes. Marine Chemistry. 2004;**89**:273-287

[13] Laane RWPM, Kramer KJM. Natural fluorescence in the North Sea and its major estuaries. Netherlands Journal of Sea Research. 1990;**26**:1-9

[14] Deng Z, He Q, Yang Q, Lin J. Observations of in situ flocs characteristics in the Modaomen Estuary of the Pearl River. Haiyang Xuebao. 2015;**37**(9):152-161. (In Chinese with English abstract)

[15] Chen ZQ, Li Y, Pan JM. Distributions of colored dissolved

organic matter and dissolved organic carbon in the Pearl River Estuary, China. Continental Shelf Research. 2004;**24**:1845-1856

[16] Callahan J, Dai MH, Chen RF, Li XL, Lu ZM, Huang W. Dissolved organic matter in the Pearl River Estuary, China. Marine Chemistry. 2004;**89**:211-224

[17] Hong HS, Wu JY, Shang SL, Hu CM. Absorption and fluorescence of chromophoric dissolved organic matter in the Pearl River Estuary, South China. Marine Chemistry. 2005;**97**:78-89

[18] Blough NV, Del Vecchio R. Chromophoric dissolved organic matter (CDOM) in the coastal environment. In: Hansell D, Carlson C, editors. Biogeochemistry of Marine Dissolved Organic Matter. San Diego, CA: Academic Press; 2002. pp. 509-546

[19] Jerlov NG. Optical Oceanography. New York: Elsevier; 1968

[20] Bricaud A, Morel A, Prieur L. Absorption by dissolved organic matter of the sea (yellow substance) in the UV and visible domains. Limnology and Oceanography. 1981;**26**(l):43-53

[21] Carder KL, Steward RG, Harvey GR, Ortner PB. Marine humic and fulvic acids: Their effects on remote sensing of ocean chlorophyll. Limnology and Oceanography. 1989;**34**(1):68-81

[22] Green SA, Blough NV. Optical absorption and fluorescence properties of chromophoric dissolved organic matter in natural waters. Limnology and Oceanography. 1994;**39**(8):1903-1916

[23] Stedmon CA, Markager S, Kaas H. Optical properties and signatures of chromophoric dissolved organic matter (CDOM) in Danish coastal waters. Estuarine, Coastal and Shelf Science. 2000;**51**(2):267-278

[24] Braslavsky SE. Glossary of terms used in photochemistry, 3rd edition (IUPAC Recommendations 2006). Applied Chemistry. 2007;**79**:293-465

[25] Nelson NB, Siegel DA, Michaels AF. Seasonal dynamics of colored dissolved material in the Sargasso Sea. Deep Sea Research, Part I. 1998;**45**:931-957

[26] Zaneveld JRV, Kitchen JC, Bricaud A, Moore CC. Analysis of in-situ spectral absorption meter data. In: Gilbert GD, editor. Ocean Optics XI. San Diego: International Society for Optics and Photonics; 1992. pp. 187-200

[27] Miller RL, Belz M, Del Castillo C, Trzaska R. Determining CDOM absorption spectra in diverse coastal environments using a multiple pathlength liquid core waveguide system. Continental Shelf Research. 2002;**22**:1301-1310

[28] Nelson NB, Siegel DA, Carlson CA, Swan C, Smethie WM, Khatiwala S. Hydrography of chromophoric dissolved organic matter in the North Atlantic. Deep-Sea Research Part I: Oceanographic Research Papers. 2007;**54**:710-731

[29] Röttgers R, Doerffer R. Measurements of optical absorption by chromophoric dissolved organic matter using a point-source integrating-cavity absorption meter. Limnology and Oceanography: Methods. 2007;**5**:126-135

[30] Helms JR, Stubbins A, Ritchie JD, Minor EC, Kieber DJ, Mopper K. Absorption spectral slopes and slope ratios as indicators of molecular weight, source, and photobleaching of chromophoric dissolved organic matter. Limnology and Oceanography. 2008;**53**(3):955-969

[31] Wong LA. A model study of the circulation in the Pearl River Estuary (PRE) and its adjacent coastal waters: 2. Sensitivity experiments. Journal of Geophysical Research. 2003;**108**:3157

[32] Dong L, Su J, Ah Wong L, Cao Z, Chen JC. Seasonal variation and dynamics of the Pearl River plume. Continental Shelf Research. 2004;**24**:1761-1777

[33] Miller WL, Moran MA. Interaction of photochemical and microbial processes in the degradation of refractory dissolved organic matter from a coastal marine environment. Limnology and Oceanography. 1997;**42**(6):1317-1324

[34] Ramond PA, Spencer RGM. Riverine DOM. In: Hansell D, Carlson C, editors. Biogeochemistry of Marine Dissolved Organic Matter. 2nd ed. San Diego, CA: Academic Press; 2015. pp. 509-533

[35] Dalzell BJ, Minor EC, Mopper KM. Photodegradation of estuarine dissolved organic matter: a multi-method assessment of DOM transformation. Organic Geochemistry. 2009;**40**:243-257

[36] Fichot CG, Benner R. The spectral slope coefficient of chromophoric dissolved organic matter (S275-295) as a tracer of terrigenous dissolved organic carbon in river-influenced ocean margins. Limnology and Oceanography. 2012;**57**(5):1453-1466

[37] Cao F, Miller WL. A new algorithm to retrieve chromophoric dissolved organic matter (CDOM) absorption spectra in the UV from ocean color. Journal of Geophysical Research, Oceans. 2015;**120**:496-516